FINAL REPORT

FOR NASA/MSFC CONTRACT NO. NAS8-32527

BENT CRYSTAL X-RAY TOPOGRAPHY

August 1978

by

D.L. Parker

Texas A&M University

Electrical Engineering Department

Institute for Solid State Electronics

College Station, Texas 77843

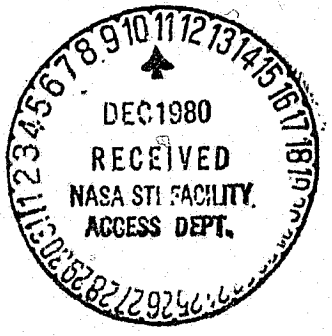

FINAL REPORT

FOR NASA/MSFC CONTRACT NO. NAS8-32527

BENT CRYSTAL X-RAY TOPOGRAPHY

August 1978

by

D.L. Parker

PREPARED FOR

National Aeronautics and Space Administration

George C. Marshall Space Flight Center

Marshall Space Flight Center, Alabama 35812

Texas A&M University

Electrical Engineering Department

Institute for Solid State Electronics

College Station, Texas 77843

Abstract

This report describes an improved version of the Television X-ray Topographic Camera System constructed by the Institute for Solid State Electronics at Texas A&M University under NASA Contract NAS 8-32527. The system differs from the previous system in that it will incorporate the x-ray TV imaging system and has a new semi-automatic wafer loading system. Also the x-ray diffraction is in a vertical plane. This feature makes wafer loading easier and will make the system compatible with any commercial x-ray generating system.

This report also includes example topographs and results obtained from a study of the diffraction contrast variation with impurity concentration for both boron implanted and boron diffused silicon.

TABLE OF CONTENTS

I. Introduction

The bent wafer x-ray topographic camera was conceived and developed under NASA contract NAS8-26379 and NASA obtained US Patent Number 4,078,175 on the apparatus in March of 1978. The work performed under this contract, NAS8-32527, had three objectives:

1. the design and construction of a new x-ray topographic camera system featuring operator safety and high throughput.
2. the development of live TV system for use with this camera.
3. the exploration of the use of x-ray topography for determining diffused and implanted impurity concentration.

The purpose of this investigation was to develop an x-ray topographic system suitable for use in a semiconductor processing facility for process control.

II. The TV X-Ray Topography System

The Television X-Ray Topographic Camera is made up of three main parts: the Wafer Chuck Assembly, TV Camera Support Arm and X-Ray Beam Tube. The Camera System is constructed primarily of Aluminum and has overall dimensions: 31" X 12" X 22". It is supported by a base of 1" Aluminum with three height, level adjustment screws.

The Wafer Chuck Assembly supports the wafer that is to be bent while it is rotated and tilted to the proper angle with respect to the x-ray beam. The Wafer Chuck is made to contain a 3.5" diameter chuck to properly bend up to a 3" diameter wafer. The wafer and chuck are held in place and bent by a vacuum controlled by a partial vacuum regulator. A vacuum slip ring is used to allow a full 360° rotation in either direction. Detail of the Wafer Chuck with a 3" diameter Silicon wafer and a plexiglass chuck is shown in Photograph 1. The plexiglass chuck must be shaped such that when the proper vacuum is applied, the chuck will be spherically deformed. The Wafer Chuck is rotated by the Chuck Drive stepping motor. A microswitch acts as a rough angle position indicator lighting a lamp every 15° of rotation. The drawings on page 16 show the size and shape of the Wafer Chuck Assembly. The drawing on the right shows the Wafer Chuck, Chuck Drive stepping motor and the angle position indication. The angle of tilt between the wafer and the x-ray beam is adjusted with a stepping motor driving a cam which through a lever arm varies the angle of the Wafer Chuck Assembly. Details of the lever arm and cam can be seen in the drawing on the left of page 13 and in Photograph 2. The tilt angle of the Wafer Chuck Assembly can be read on a dial. This dial is shown on the left of Photograph 3 and in the lower left drawing on page 12. Photograph 4 shows the Wafer Chuck in position for x-ray diffraction. The control unit drives

the chuck and tilt stepping motors independently. Direction of stepping motor is determined by a paddle switch. Lamps indicate which stepping motor is being driven and in which direction. A pneumatic actuator tilts the Wafer Chuck Assembly into the horizontal loading position. Photograph 2 show the vacuum actuator, and a Silicon wafer in the loading position is shown in Photograph 1.

The TV Camera Support Arm supports the TV Camera, a light tight box with a flourescent screen, and film cassette. The angle of the TV Support Arm has a manual adjustment by means of a hand screw over a range of 30°. The TV Support Arm with the TV Camera mounted is shown in Photographs 5 and 6. Also in Photograph 6, the hand screw is shown above the X-ray Beam Tube. Drawings on pages 11,12, and 13 show that support arm from different perspectives. The dial shown in the top of Photograph 3 indicates the angle of the TV Support Arm. The window for this dial can also be seen in the lower left drawing on page 12. The light tight box, flourescent screen and film cassette are not shown in the drawings or photographs. The slot for the film cassette is shown above the Wafer Chuck in Photograph 4 and in the drawing on the right of page 12.

The X-ray Beam Tube is constructed of Aluminum and lined with lead. At the end of the beam tube there is an adjustable adapter to connect to the shutter of the x-ray machine. The beam tube, adapter, and x-ray shutter assembly are shown in Photograph 7. Drawings on pages 11, 12, and 13 show details of the adapter. The X-ray Beam Tube also contains three inserts to modify the X-ray beam: an adjustable slit assembly, an X-ray filter holder, and a variable elliptical collimator. Details of these three inserts are shown in the drawings on pages 14 and 15. Details of the adjustable slit and elliptical collimator are shown in Photographs 8 and 9. The drawings on

page 11 and the lower left page 12 show the location along the beam tube for these inserts.

The Television X-Ray Topographic Camera System is shown connected to the X-Ray machine in Photograph 10. The drawing on page 11 shows a perspective view of the Camera System.

The camera may be operated remotely by three controls: 1) chuck tilt, 2) chuck rotation, and 3) partial vacuum. The operator adjusts these controls to obtain the best possible image on the realtime TV monitor. Once this is established, the x-rays are then turned off and the photographic plate cassette is inserted in front of the TV camera system to make a hard copy exposure. The TV system greatly simplifies the alignment procedures and assures a good hard copy every time. Multiple reflections (where two images are recorded superimposed with a fixed camera setting) is a frequent problem when a radiation detector is used for the initial camera settings. This problem can be completely avoided with the TV system. The TV system is also very useful for exploring unfamiliar material for a useful x-ray reflection.

The TV monitor image, at present, has too much noise and too little resolution to be useful in wafer inspection. The noise is due to the extremely low light level produced in the phosphors by the diffracted x-ray beam. The resolution limit is primarily due to the phosphor grain size, thickness and noise. The camera and monitor system has adequate resolution to observe severe lattice damage. The Prineton Electronic Products PEP500 Lithicon Image Storage Unit significantly improves the image noise when it is used in the integration mode. However, the integration time required to produce a useful video image is about one minute and the resolution is still inadequate for direct wafer inspection. The main application of the PEP500

has been the storage of one integrated image for comparison with subsequent live images.

A new vacuum chuck design was developed in the last stages of this contract. The original concept of a spherically machined rigid vaccum chuck has been adandoned in favor of the flat surface elastically deformable chuck. The rigid chuck suffered from two disadvantages: 1) the partial vacuum required to force some heavily processed wafers to conform to the chuck shape sometimes caused sever dimpling in the wafer and 2) the typical orientation variations from wafer-to-wafer requires significantly different curvature for a camera with a fixed chord length. On the other hand the flat surface deformable chuck with a tapered back did not give uniform results either. The curvature of some wafers could be adjusted almost perfectly while other wafers of the same size and cut gave poor results. The difficulty lies in the distribution of defects in the wafer itself. This affects the symmetry of the stiffness of the wafer-chuck combination. The new design is simply a combination of these two designs using the advantages of both. The chuck surface is machined to a radius of curvature somewhat greater than that which is ultimately desired the partical vacuum is then adjusted to complete the bending while monitoring the realtime video monitor image.

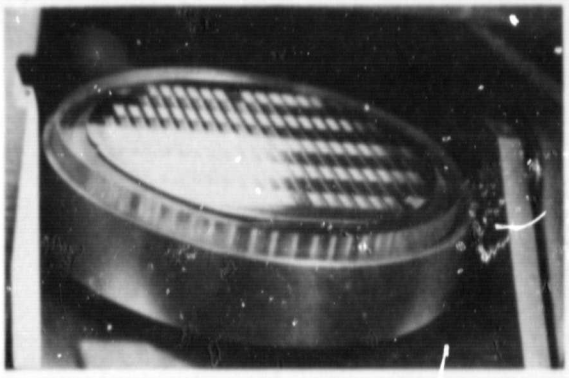

Photograph 1: Detail of Wafer Chuck with a three inch silicon wafer and plexiglass chuck.

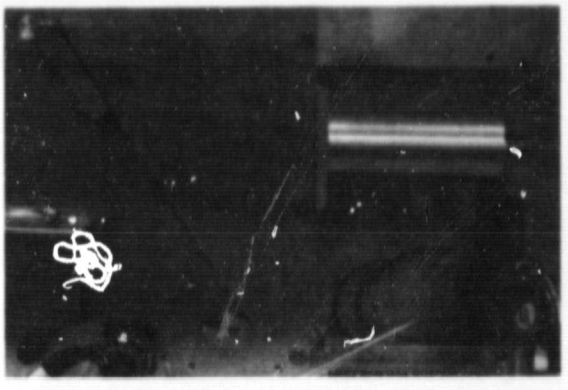

Photograph 2: Cam and lever arm for wafer tilt, vacuum solenoid, and piston assembly.

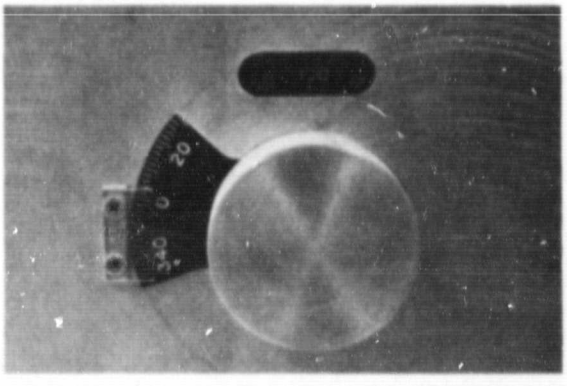

Photograph 3: Angle dials showing tilt of TV Support Arm (above) and Wafer Chuck Assembly.

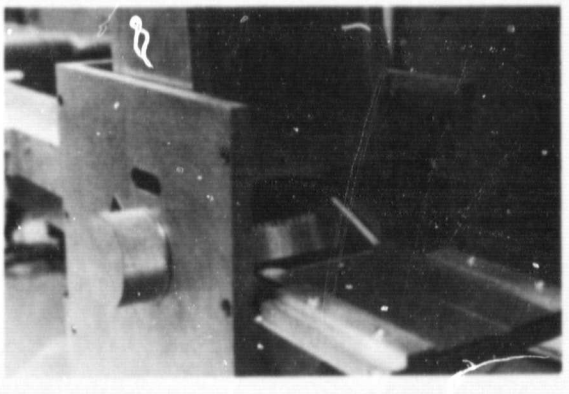

Photograph 4: Wafer Chuck in position for diffraction. Also slot for the film cassette is shown.

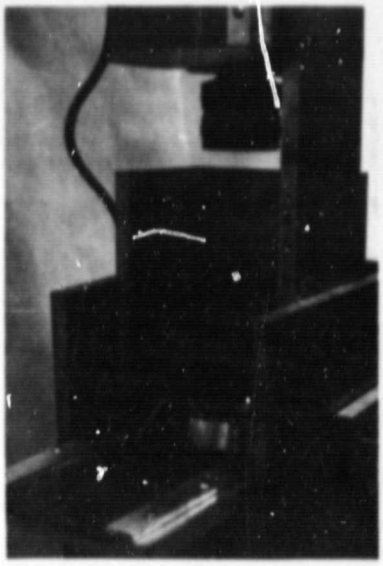

Photograph 5: TV camera mounted on TV Support Arm.

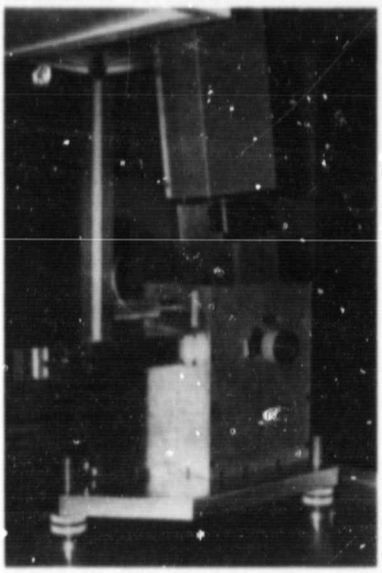

Photograph 6: Perspective view showing TV Support Arm and hand screw for angular adjustment of Support Arm.

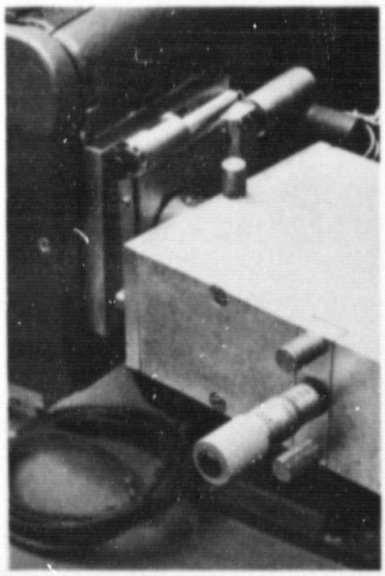

Photograph 7: Detail of X-Ray shutter, adjustable slit, and Beam Tube Adapter.

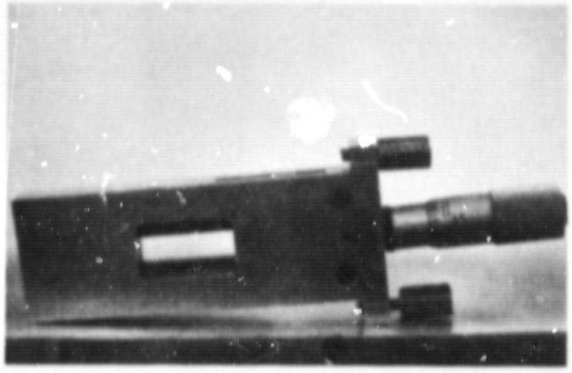

Photograph 8: Adjustable Slit Assembly.

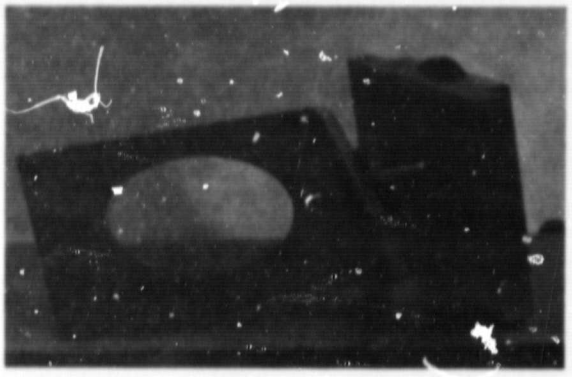

Photograph 9: Variable elliptical Collimator.

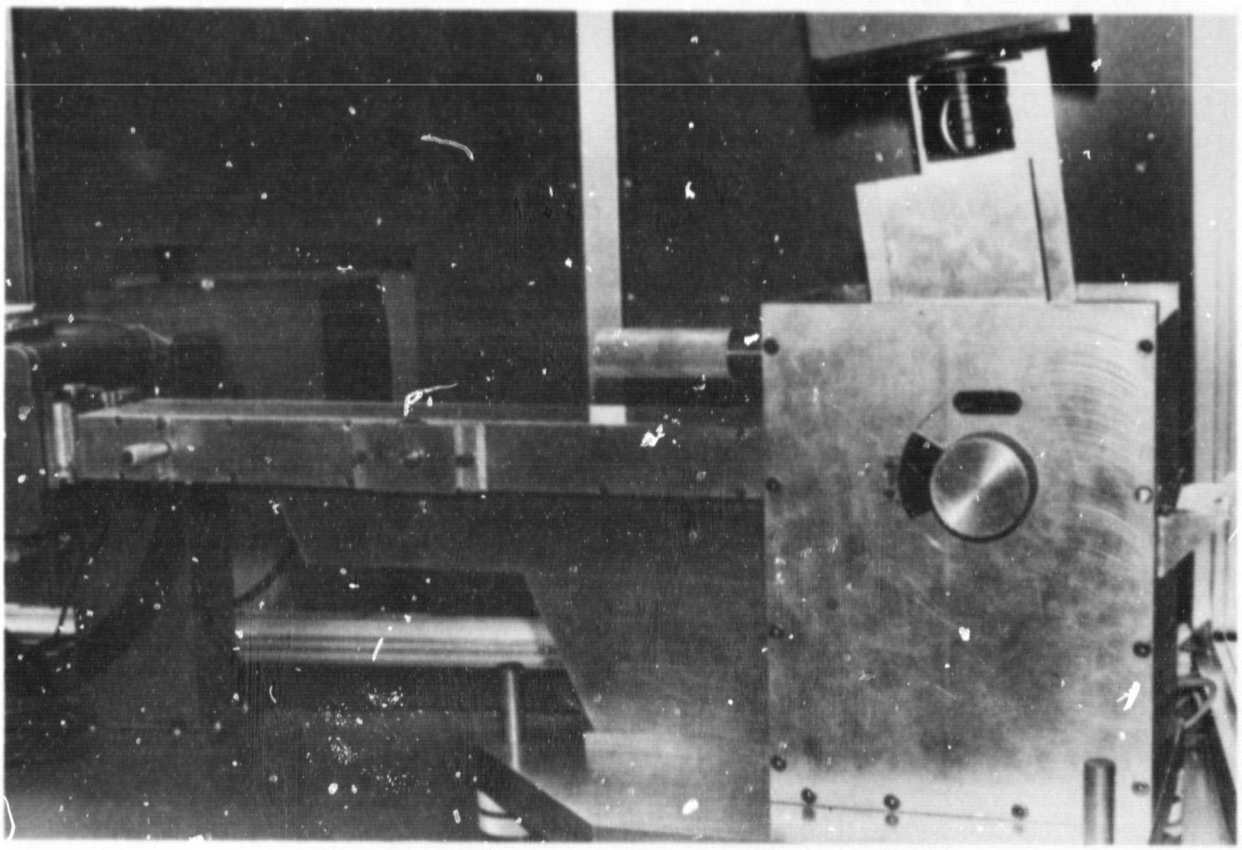

Photograph 10: TV Topographic Camera System with X-Ray Machine

TELEVISION X-RAY TOPOGRAPHIC CAMERA

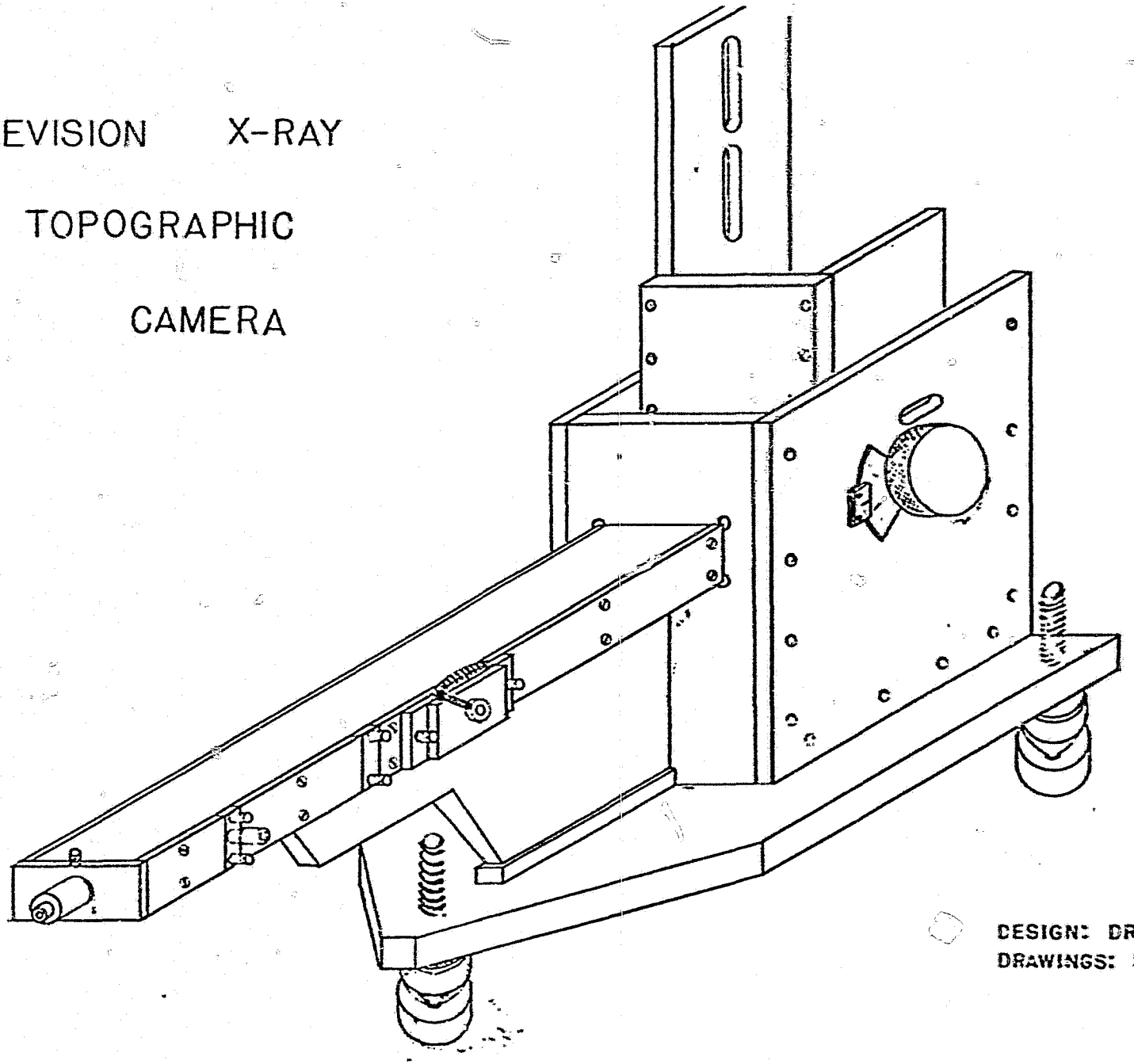

DESIGN: DR. D. L. PARKER
DRAWINGS: S. FAIRCHILD

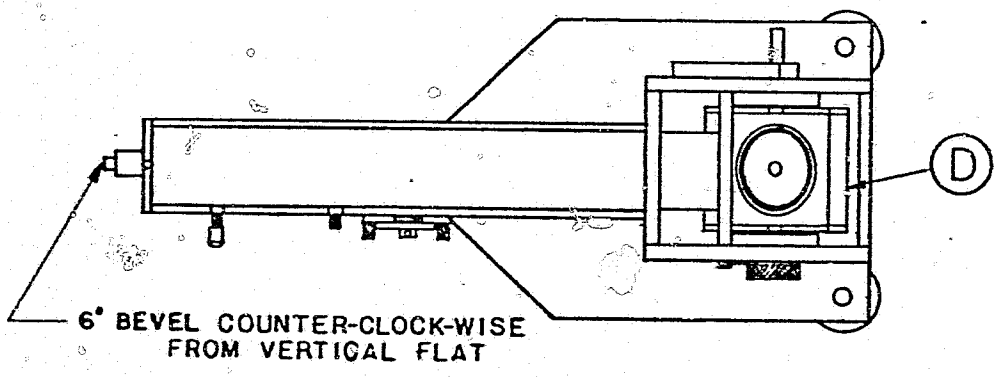

NOTE: SUPPORT ARM SHOWN IN 90° POSITION; CAPABLE OF A +20°, -10° ANGULAR TILT AS INDICATED.

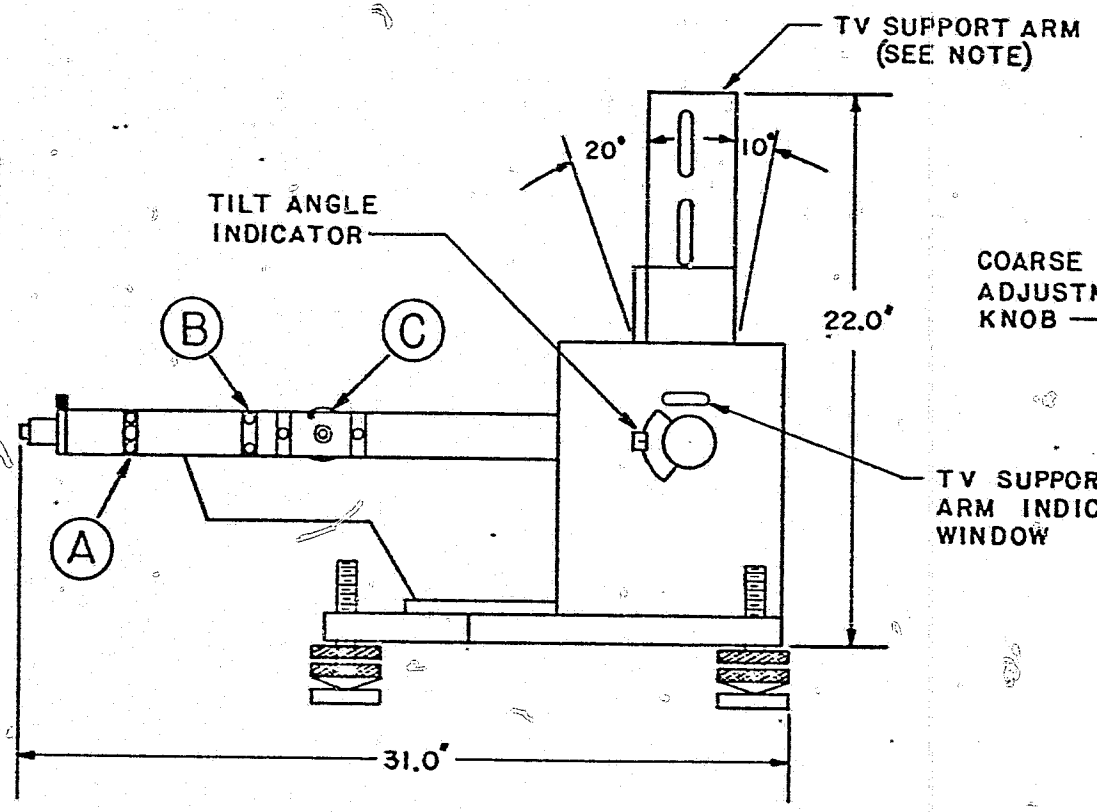

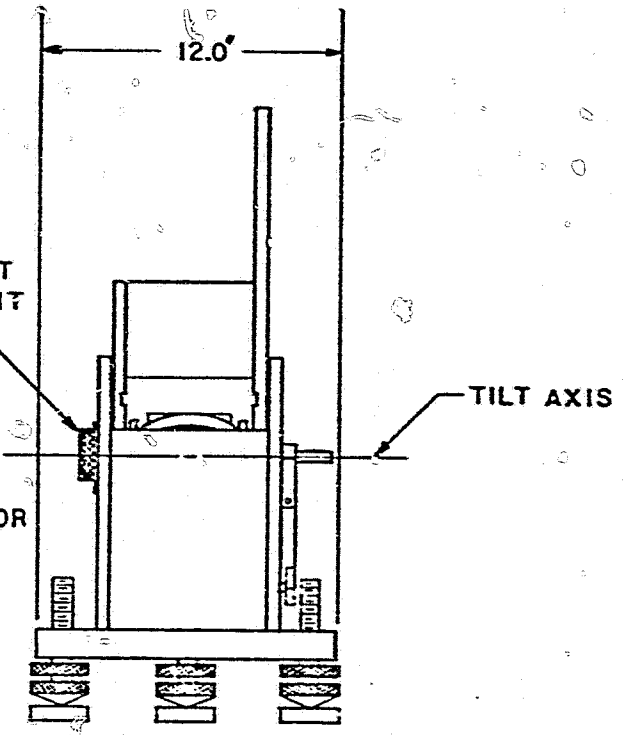

ORIGINAL PAGE IS
OF POOR QUALITY

ORIGINAL PAGE IS
OF POOR QUALITY

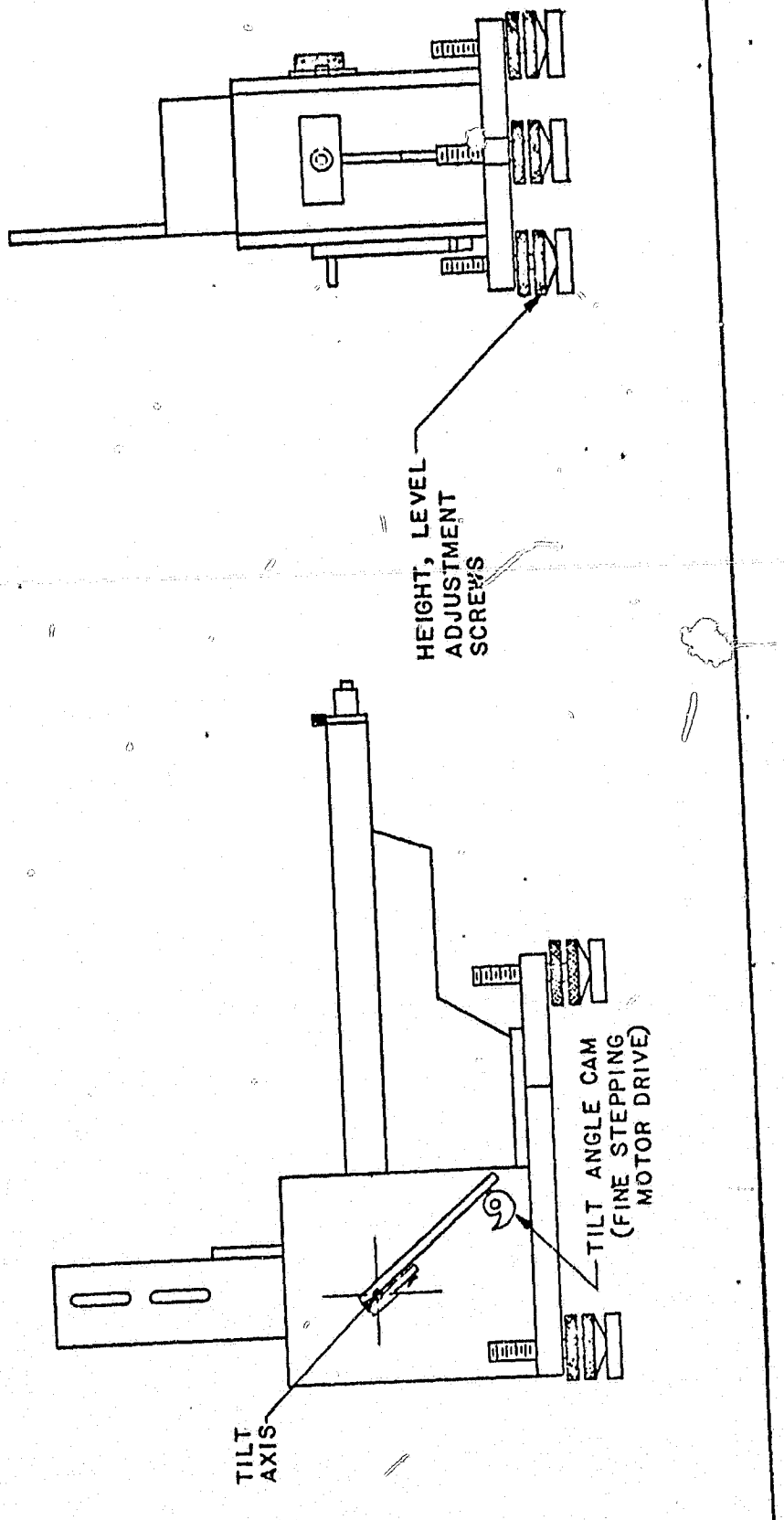

ADJUSTABLE SLIT ASSEMBLY

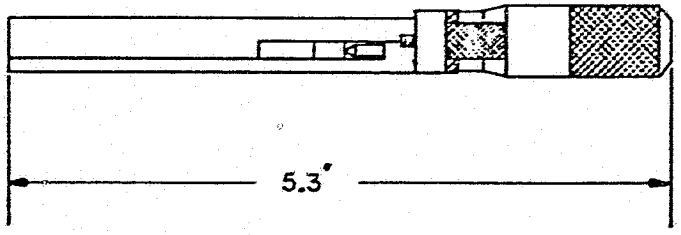

(A)

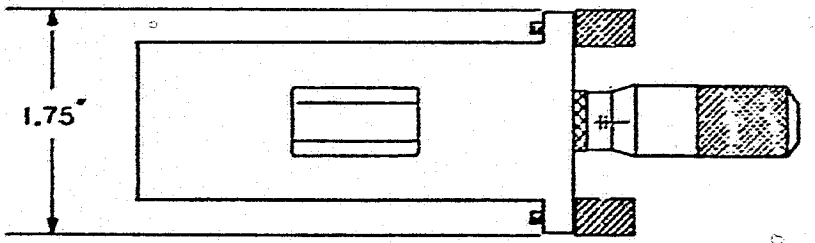

X-RAY FILTER HOLDER

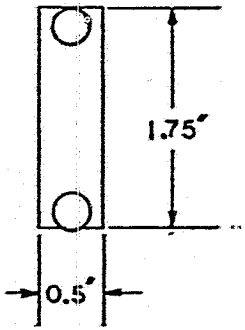

(B)

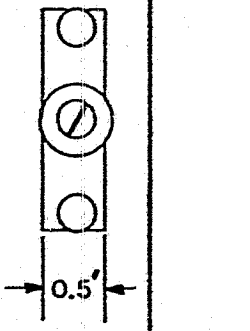

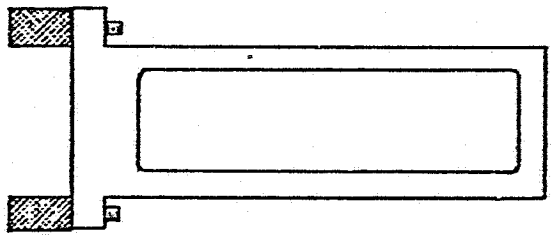

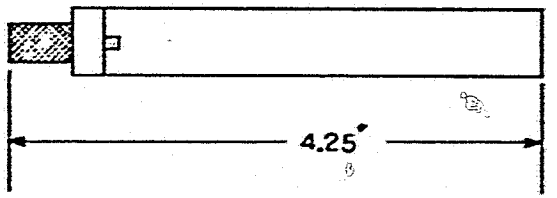

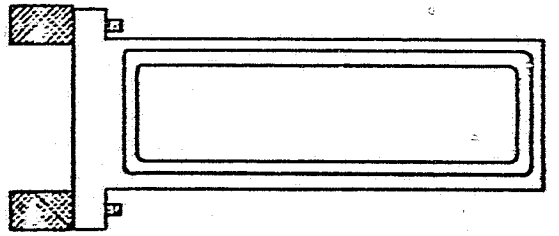

VARIABLE ELLIPTICAL COLLIMATOR

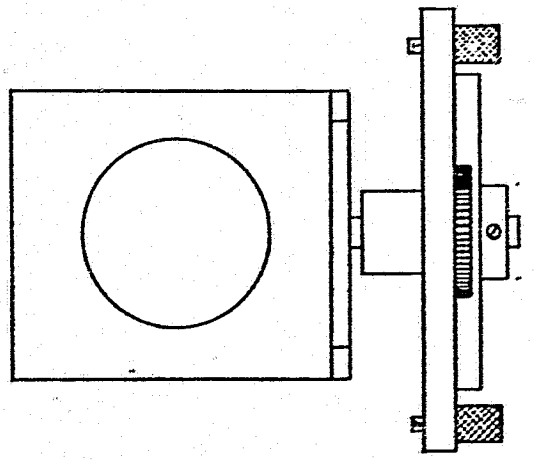

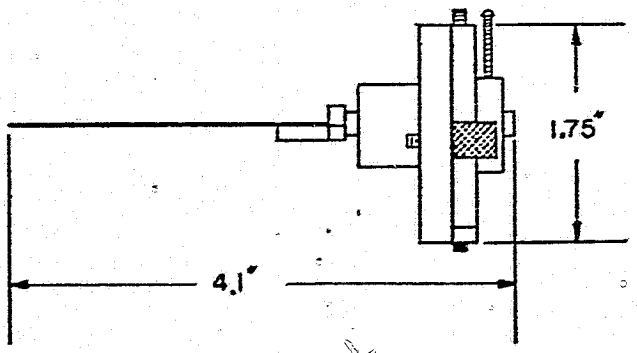

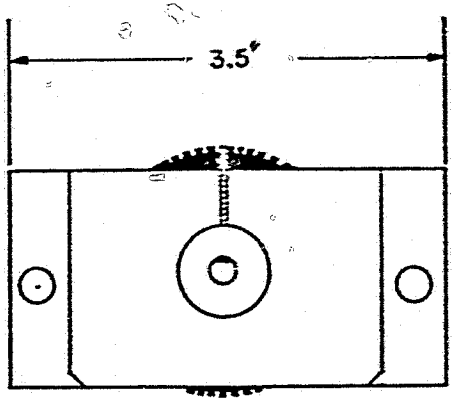

WAFER CHUCK ASSEMBLY

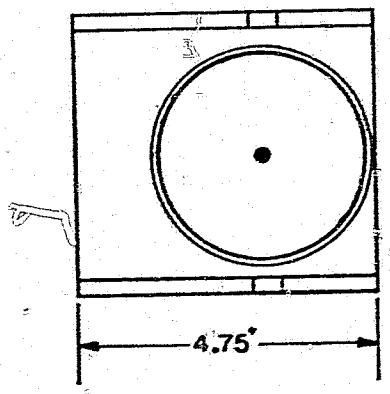

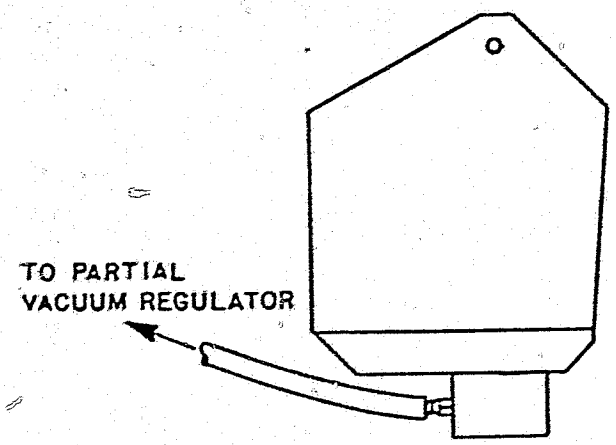

(D)

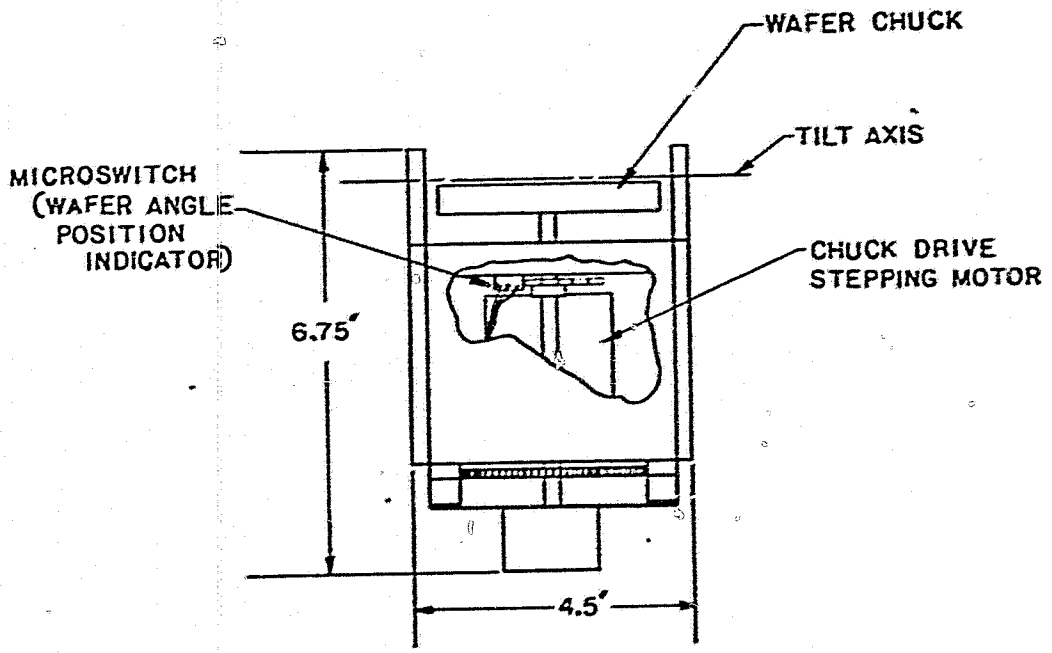

III. The Effects of Impurity Concentration on Image Contrast

The purpose of this study was to explore the feasibility of using the measured diffracted x-ray beam intensity to determine the impurity concentration in a region of the wafer after a given deposition or implant step. A special mask set was constructed for this purpose consisting of 1/8th inch wide rings concentric with the wafer. The completely diffused wafer has the form of a bullseye pattern with alternate rings receiving a different diffusion (sheet resistivity and/or junction depth). A separate ring between each diffused ring was left undiffused to serve as a standard background. The bullseye pattern could then be scanned by the x-ray beam across any diameter. A special geniometer attachment was constructed to allow the detector to be tilted out of the normal diffraction plane which is perpendicular to the wafer surface. This configuration allows the x-ray incident angle to be varied continuously from some maximum angle down to zero grazing incidence for several different diffracting conditions. The hope was that at small angles of incidence, the beam would not penetrate through the diffused layer and thus higher contrasts and corresponding higher sensitivities would result.

A considerable amount of data was taken on a variety of diffused and implanted wafers with a bullseye pattern. This data consisted of counts measured with a Sodium Iodide x-ray detector as the incident x-ray beam illuminated first diffused then nondiffused rings in the bullseye pattern. A ratio was taken of the number of counts in a diffused region to the number of counts in a nondiffused region. The ratio of these counts did increase up to a point as the incident angle was decreased; however, the gain in sensitivity was not considered sufficient to justify the added complexity i.e. the requirement that the defector tilt out of what is ordinarily the central scattering plane. The extra sensitivity can be achieved with standard

diffracting conditions by simply making slightly longer counts for improved statistics.

Impurity sources for the diffusion part of these experiments were both boron (solid source) and phosphorus (liquid source). As expected, the count ratios for the boron impurity is greater than for phosphorus with the same sheet resistivity. We were unable to obtain sheet resistivities less than about 5 ohms per square with boron without considerable slip damage regardless of the care used in processing.

The ratios observed in the counting data ranged from 2.4 to one for a heavy boron diffusion down to one to one for very light phosphorus diffusions. No attempt was made to "calibrate" this technique due to the sheer size of the task and to the time required to construct the television x-ray topography system. However, the following useful qualitative information was obtained:

1) Implanted boron produces no contrast in the x-ray images until after the anneal step.
2) The image contrast produced by boron diffusion increases noticeably after the drive in step.
3) Starting material defects are more easily identified in the diffused (or implanted) regions. This indicates clustering of the boron at the defect sites.
4) There is no significant difference in ratio produced by implanted and diffused boron when sheet resistivities and junction depths are comparable.
5) Boron produces a higher count ratio than phosphorus impurities when sheet resistivities are comparable.

The data to support these conclusions are in tabular form and, of course, many x-ray topographs. Two of the more significant topographs are included in this report with processing details on one of the wafers.

Wafer I-10 After Boron Diffusion

Data taken with 20-mil window width, 35 kV acceleration potential and 10 MA tube current.

	Region	Counts in 100 sec.	Ratio
1	Starting Matl.	103523	1.12
2	Diffused Ring	115671	1.15
3	Starting Matl.	100717	
4	Starting Matl.	97510	1.18
5	Diffused Ring	115377	1.12
6	Starting Matl.	106099	

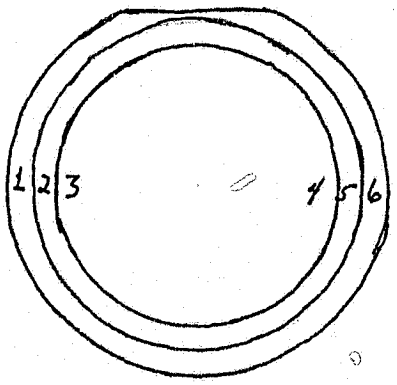

TYPICAL DATA FOR THREE REFLECTIONS OF A DIFFUSED WAFER

Reflection	(440)	(422)	(333)
Incident Angle	18°	24.5°	47.48°
2θ	106.71°	88.03°	94.96°
Position		Counts in 10 seconds	
0.0	1912	10187	10014
0.1	12564	15693	9951
0.2	22742	23704	16752
0.3	17057	10461	9290
0.4	12045	10312	9712
0.5	12068	10779	9959
0.6	12244	10658	10054
0.7	12553	10898	10099
0.8	12024	11044	10240
0.9	12489	11041	10420
1.0	12207	10982	10159
1.1	12863	10815	10366
1.2	12289	10909	10030
1.3	12129	10958	10178
1.4	11788	10885	10100
1.5	12102	10486	9793
1.6	12020	10352	9945
1.7	11859	21566	12080
1.8	22266	21448	16152
1.9	12029	10655	10360

I-2 PROCESSING STEPS

Starting Material - (III) Silicon 2 inch wafer from Semiconductor Products Incorporated. Phosphorous doped to 15-17Ω-cm.

First Oxidation - 1 hour at 1000°C in steam. Inner and outer ring windows cut.

Boron Implant - 10 hour implant into inner and outer ring windows. Current started at 1 1/2 μa and drifted down to 0.1μa. Total boron charge unknown.

2nd Oxidation anneal- 1 hour at 1000°C in steam. 2nd (middle) ring window cut.

Boron Deposition - Boron nitride Grade A wafer source. 1 hour at 1000°C followed by 750°C steam deglaze.

Final drive in - 900 -- 1150° ramp in O_2 (30 min)
15 min. in steam at 1150°C
30 min. in N_2 at 1150°C

All oxide was stripped off and the junction depths were measured by the groove and stain method.

Sheet resistivities { Implant rings 8.4
Diffused ring 10.6

Junction depths { Implant rings 3 microns
Diffused ring 4 microns

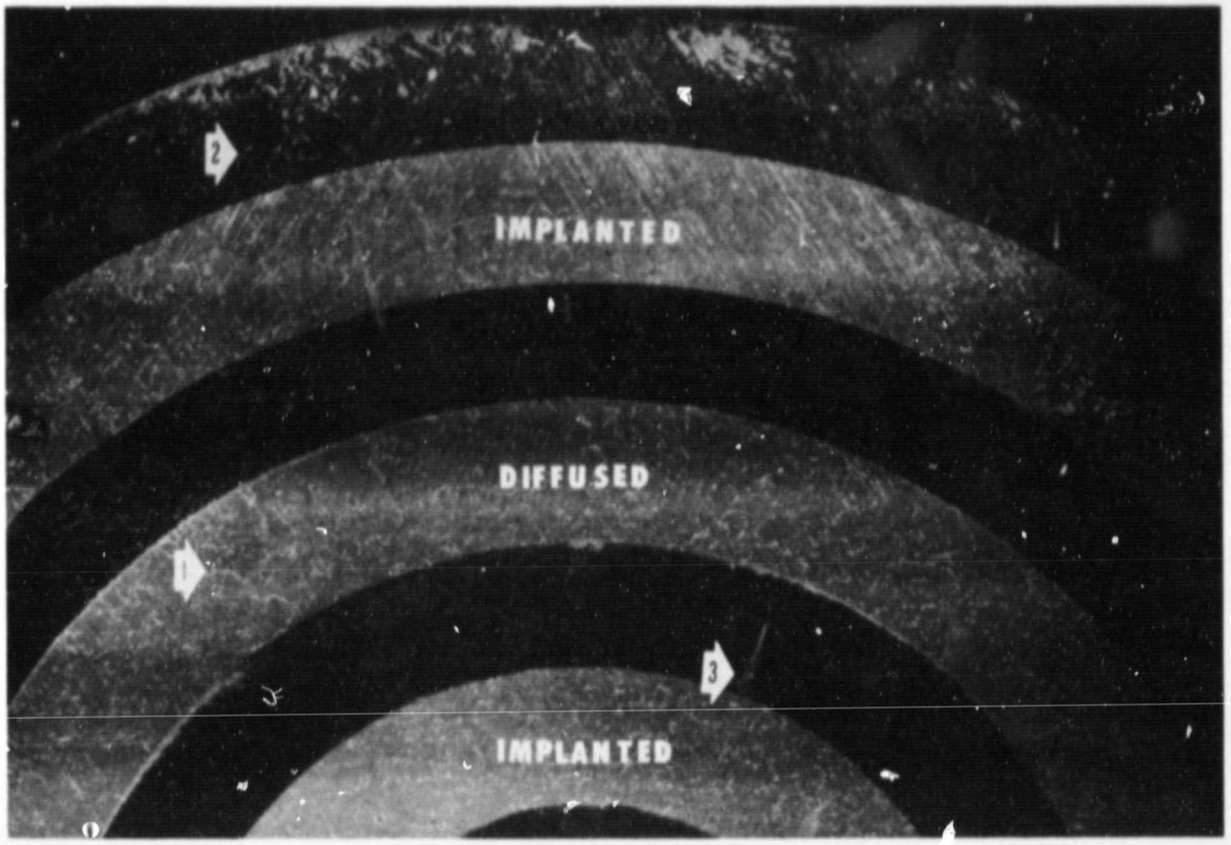

Figure 1: X-ray topograph of a typical wafer (I-2) with bullseye pattern

The wafer shown received the same boron implant in the inner and outer rings. The middle ring received a boron diffusion. The sheet resistivities and junction depths of all three rings are comparable and are given with the processing information. The contrast due to boron impurities is quite distinct in this topograph. Also a number of defects can be seen:

1. Starting material defects (random curly pattern)
2. Process induced slip damage (straight lines near the wafer edge)
3. Masking errors (photoresist lifting)

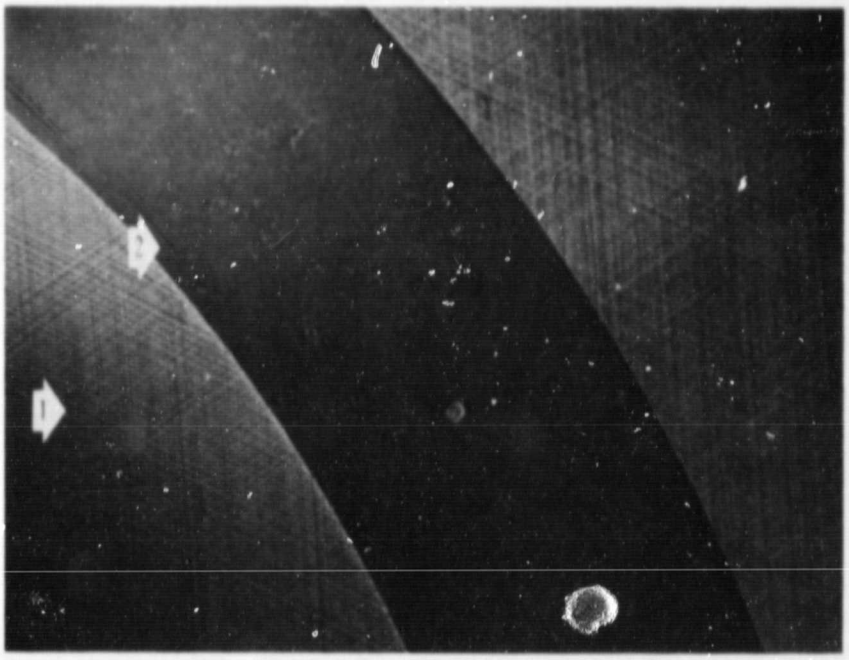

Figure 2: X-ray topograph of 2 inch silicon wafer.

The topograph was made after a heavy boron diffusion. The sheet resistivity is about one ohm per square and the junction depth is about three microns. The extreme slip damage (shown by arrow one) is typical with high boron impurity concentration. Also note that high stress at the window edge causes dislocations to be propogated into nondiffused regions (arrow two). A number of point defects are visable in the nondiffused region.

IV. Other Applications of X-ray Topography in Semiconductor Process Control

There is currently an explosion of interest in the use of laser radiation in semiconductor processing. This radiation is strongly absorbed in semiconductor materials and can be used to produce highly localized heating. The advantages are obvious. The ability of the laser beam to anneal and activate implanted material has already been widely demonstrated. Among the proposed processing steps are 1) localized diffusion of dopants, 2) epitaxial growth from amorphous or polycrystal layers and 3) maskless processing.

We have recently demonstrated the ability of a laser beam to anneal process induced defects with x-ray topography. Severe lattice damage was induced in a two inch (111) silicon wafer with a rapid thermal cycle. The wafer was placed on a flat horizontal quartz boat which has a hole under the wafer. A rapid thermal cycle produces severe slip damage in the region over the hole. The wafer was then scanned with several passes of Nd:YAG laser radiation at various power levels. The laser was scanned thru the region with the most severe lattice damage.

The two x-ray topographs included in this section were then made. These topographs demonstrate the ability of the laser to repair process induced defects and the ability of x-ray topography to illustrate the extent of the damage and the repair; even to give an estimate of the depth of the repair.

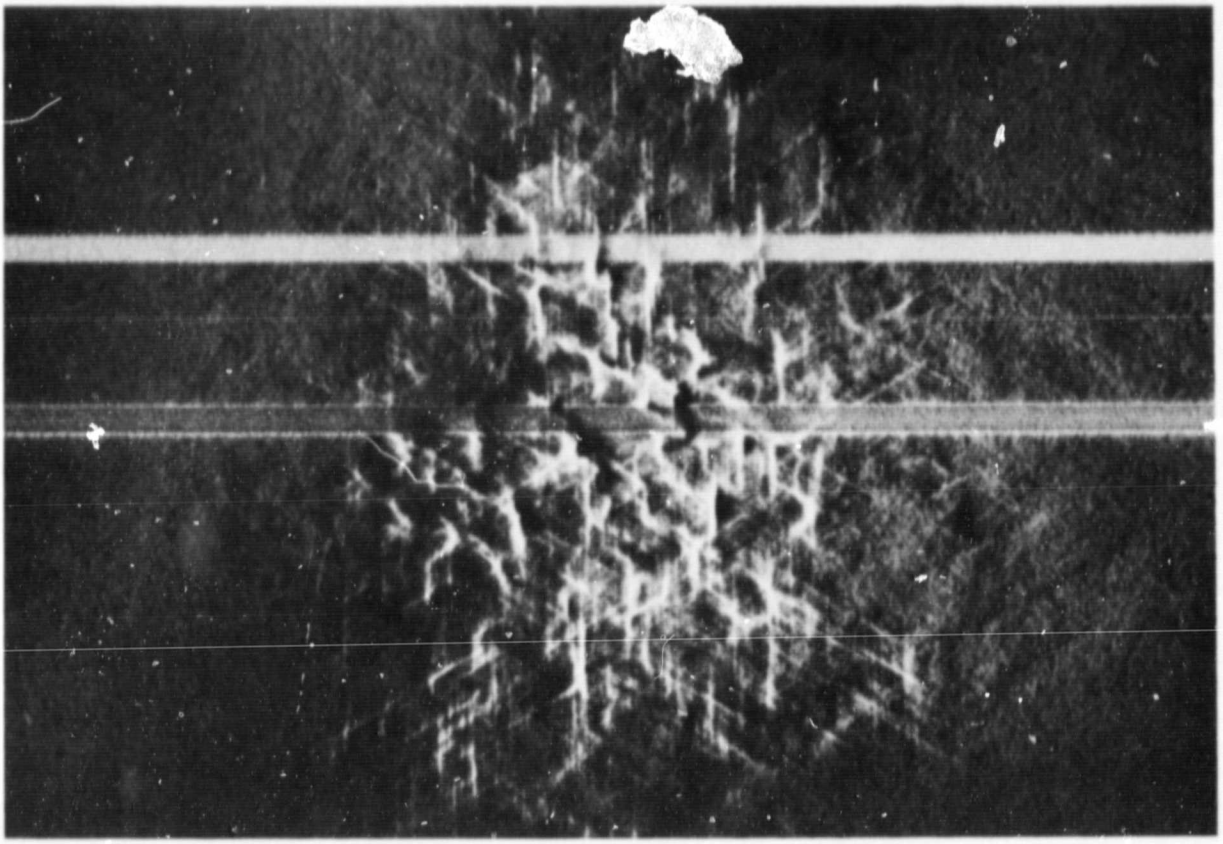

Figure 3: X-ray topograph of the laser treated (111) Silicon wafer (440 reflection)

The topograph shown was made with $CuK_{\alpha 1}$ radiation. To obtain this (440) reflection, the x-ray incidence angle must be about 18^{o} to satisfy the Bragg Law for reflection. The x-ray radiation at this angle penetrates only about 25 microns below the silicon surface. Thus we conclude that all of the defects visible in this topograph are in the first 25 microns of the surface.

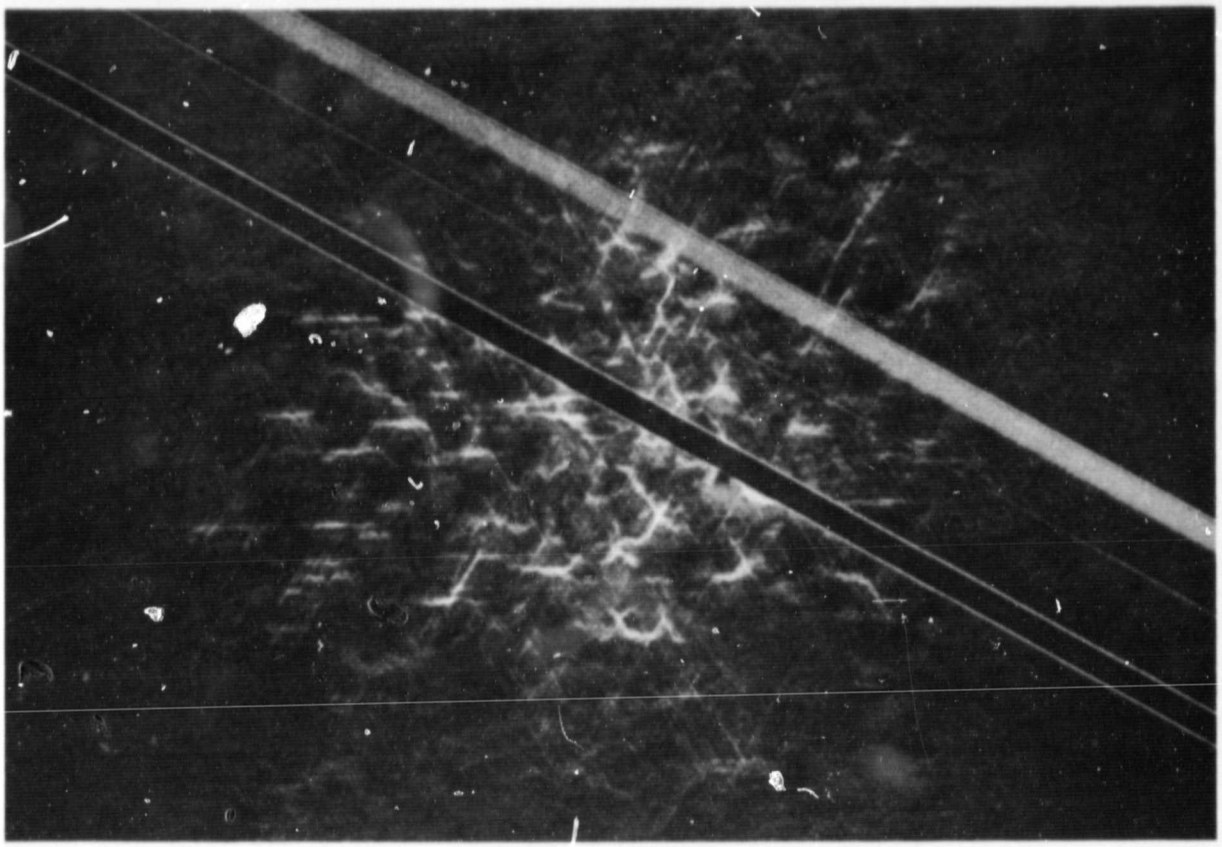

Figure 4: X-ray topograph of the laser treated (111) silicon wafer (511 reflection)

This (511) reflection x-ray topograph was made from the same (111) silicon wafer as the topograph show in Fig. 3. Again $CuK_{\alpha 1}$ x-ray radiation was used. This configuration requires the x-ray incidence angle to be about 8^{o}. At this angle $CuK_{\alpha 1}$ radiation only penetrates about 10 microns below the surface of the wafer. Note that the darker laser scan is very clean when compared to the same scan with the (440) reflection in Fig 3. We conclude that the effective depth of this particular laser anneal is between 10 and 25 microns.

V. Summary and Conclusions

The most significant development made under this contract has been the live TV monitoring capability. This development makes the use of the camera fast and simple even for a relatively untrained operator. The new chuck design appears to offer the best compromise amoung speed, performance, convienience, and versatility.

The new model of the bent wafer camera designed and constructed under this contract has three distinct advantages over the previous model:

1. shielding and interlock protection reduces the risk of accidental radiation exposure for the operator
2. the camera is compatable with any commerical diffraction x-ray generator
3. the new model is more compact and portable.

The time required for wafer loading, unloading and alignment is now negligible compared to the time required for exposure, darkroom processing, and topograph interpretation.

We feel that the feasability of using the diffracted x-ray beam intensity to estimate total dopant content in silicon has been demonstrated, at least in principle. Any practical commercial application of this technique; however, will require rather sophisticated digital image processing equipment.

The TV system in its present state of development is completely adequate for the initial wafer alignment. The system saves considerable darkroom processing time particularly when a new lot of wafers is to be topographed. The resolution and contrast of the TV image is only adequate for detecting the most gross crystal damage however. There does not seem

to be much hope that a true live topography wafer inspection system can evolve from the present system however. The resolution is limited by the thickness and grain size of the phosphor coating used to produce the visable light image. Thinner coatings and smaller grain sizes reduce the light level to intolerable levels. It seems that a breakthrough will be required in the way an x-ray image may be converted into a video signal.

The camera has been developed to a point where it is ready for evaluation on current production wafers. This can be most easily accomplished by obtaining completely processed and probed wafers from a variety of vendors and covering a variety of device types. Defects detected in x-ray topographs of these wafers should be correlated with the yield pattern. These wafers should be selected from lots which have relatively low yields for unknown reasons if possible. It is recommended that this correlation study be done in the Institute for Solid Sate Electronics facilities for two reasons;

1. the equipment is already operational and moving the equipment would only delay the work
2. a larger variety of device types may be tested by using different vendors than would probably be done if the equipment were moved to a production facility.